

## STRUCTURAL AND OPTICAL PROPERTIES OF CdS/Cu(In,Ga)Se<sub>2</sub> HETEROSTRUCTURES IRRADIATED BY HIGH-ENERGY ELECTRONS\*

A. V. Karotki,<sup>a\*\*</sup> A. V. Mudryi,<sup>a</sup> M. V. Yakushev,<sup>b</sup>  
F. Luckert,<sup>b</sup> and R. Martin<sup>b</sup>

UDC 535.37;539.216.2

*Thin films of Cu(In, Ga)Se<sub>2</sub> (CIGS) with a Ga/(Ga + In) ratio of ~0.27 corresponding to the standard elemental composition for solar-energy transducers were grown on Mo-coated glass substrates by the Cu, In, Ga, and Se co-evaporation technique from different sources. Transmission (T), photoluminescence (PL), and photoluminescence excitation (PLE) spectra at 4.2 K were used to analyze electronic properties in the as-grown and electron-irradiated CIGS films. The band-gap energy (E<sub>g</sub>) of the CIGS films measured using both transmission and PLE methods was found to be about 1.28 eV at 4.2 K. Two deep bands in the PL spectra of the irradiated CIGS films, P<sub>1</sub> at ~0.91 eV and P<sub>2</sub> at ~0.77 eV, have been detected. These bands are tentatively associated with copper atoms substituting indium (Cu<sub>In</sub>) and indium vacancies V<sub>In</sub>, respectively, as the simplest radiation-induced defects.*

**Keywords:** Cu(In,Ga)Se<sub>2</sub>, photoluminescence, electron irradiation, defects.

**Introduction.** Fabrication of highly efficient solar cells based on Cu(In,Ga)Se<sub>2</sub> (CIGS) semiconducting films is a critical and simultaneously complicated scientific and technical problem of modern semiconducting solar energy [1, 2]. The development and improvement of the technology for preparing solar cells using CIGS compounds with the chalcopyrite structure has recently enabled efficiency records (~19.9%) to be set for all known thin-film semiconducting materials [1]. The stable operation of solar cells based on CIGS compounds that are used under ordinary terrestrial conditions and, especially, that are exposed to penetrating radiation (high-energy electrons, protons, etc.) in near-earth space orbits to an even greater extent stimulate further scientific and technological developments of semiconducting solar photovoltaics based on these materials [1–5]. Such promising developments prompt investigations that determine the criteria for radiation resistance of CIGS semiconducting compounds and solar cells based on them to the action of high-energy particles and that establish the nature of the radiation-induced defects at the atomic level [3–6]. New knowledge about the radiation physics of defects in CIGS material will indubitably assist a deeper understanding of the geometric and electronic structure of not only radiation defects but also growth defects formed during formation of CIGS thin films that determine the perfection of the material crystal structure. Herein we describe experiments that establish the nature of the radiation defects in CdS/Cu(In,Ga)Se<sub>2</sub>/Mo (CdS/CIGS/Mo) heterostructures, on which solar cells with efficiency ~12–14% are based [4, 7, 8].

**Experimental.** The studied CIGS films were sputtered onto glass substrates coated with a thin film of Mo with simultaneous co-evaporation of Cu, In, Ga, and Se using well-known technology [4, 7–9]. Layers of CdS (~50 nm thick) were deposited by the standard chemical method in the corresponding solutions. The studied CdS/CIGS/Mo/glass structures consisted of a CdS buffer layer (~50 nm), CIGS films (~1.5 μm thick), a contact layer of Mo (~0.8 μm thick), and the glass substrate (2 mm thick). The elemental composition of the films was determined by local energy-dispersive x-ray analysis (XA) and scanning Auger-electron spectroscopy (SAES) with layer-wise surface removal. The standards for measuring the optical transmission were CIGS films grown directly on glass substrates. The film struc-

\*Presented at the International Conference "Photovoltaic Science Applications and Technology-5," April 1–3, 2009, Glyndwr University, Wales, UK.

\*\*To whom correspondence should be addressed.

<sup>a</sup>Scientific-Practical Material Research Centre, National Academy of Sciences of Belarus, 19 P. Brovka St., Minsk, 220072, Belarus; e-mail: anatoli-karotki@ifftp.bas-net.by; <sup>b</sup>Strathclyde University, Glasgow, UK. Translated from Zhurnal Prikladnoi Spektroskopii, Vol. 77, No. 5, pp. 725–731, September–October, 2010. Original article submitted March 5, 2010.

TABLE 1. Elemental Composition (at %) of CIGS Thin Films from SAES and XA

Sample	Analytical method	Substrate type	Cu	In	Ga	Se	Ga/(Ga + In) ratio
1	SAES	Mo/glass	25.1	18.6	6.8	49.5	0.268
1	XA	Mo/glass	24.1	18.8	7.2	49.5	0.277
2	SAES	glass	23.0	19.9	7.1	50.0	0.263
2	XA	glass	23.0	19.9	7.4	50.0	0.271

tures and their phase compositions were determined by x-ray diffraction analysis using  $\text{CuK}\alpha$ -radiation ( $\lambda = 1.5409 \text{ \AA}$ ). Scanning electron microscopy (SEM) was used to analyze the surface morphology. CIGS films were irradiated with electrons of energy 5 MeV at doses of  $10^{16}$ – $2 \cdot 10^{18} \text{ cm}^{-2}$  with electron-beam flux  $10^{12} \text{ cm}^{-2} \cdot \text{s}^{-1}$  at temperatures  $50^\circ\text{C}$ . Optical transmission and reflectance spectra were recorded in the spectral range 200–3000 nm at 300 and 4.2 K using a Cary 500 UV-Vis-NIR dual-beam spectrophotometer or an MDR 23U monochromator with an objective mirror of focal distance  $f \sim 60 \text{ cm}$  and a diffraction grating with 600 lines/mm. Photoluminescence (PL) was measured at 4.2 K using an Ar laser at  $\lambda \sim 488 \text{ nm}$  and power  $\leq 200 \text{ mW}$ . The optical signal detectors were InGaAs *p-i-n*-photodiodes or PbS photoresist cooled to liquid-nitrogen temperature (Hamamatsu, Japan). Luminescence excitation spectra were recorded using an MDR-12 monochromator with an objective mirror of focal length  $f \sim 30 \text{ cm}$  and a tungsten-halogen lamp (400 W). Additional features of the method have been published [10].

**Discussion.** Table 1 presents the average concentrations of Cu, In, Ga, and Se in CIGS thin films grown directly on glass substrates (glass) or glass substrates coated beforehand with a deposited layer of Mo (Mo/glass) that were measured by SAES and XA. Results for XA were averaged over three measurements at different sites on the sample surface; SAES, concentration measurements at each stage of layered removal of films (20 values). Figure 1 shows an example of element distribution profiles along the CIGS film thickness (sample 1) measured using SAES. It can be seen that Cu and Se are distributed practically the same with thickness and that their concentrations decrease sharply near the boundary with the Mo layer. The Ga concentration increases slightly whereas that of In decreases as the boundary with the Mo layer is approached. The same practically uniform distribution of the elements over thickness is typical also of CIGS films on glass (sample 2). Figure 2 shows the surface morphology and a chip cross-section of the CdS/CIGS/Mo/glass heterostructure from SEM data. It can be seen that the crystallite size is  $\sim 0.3$ – $1.2 \mu\text{m}$  and is in certain instances comparable with the thickness of the CIGS layer (Fig. 2b). The SEM images demonstrate that large grains are densely packed with little porosity and that the CIGS layer adheres firmly to the Mo layer or the glass.

The x-ray diffraction studies showed that CIGS films formed on glass or the Mo layer had a single-phase chalcopyrite structure. Figure 3 shows an example of x-ray diffraction patterns of the CdS/CIGS/Mo/glass heterostructure (sample 1). It is noteworthy that reflections from the crystal lattice of the CdS layer were not observed because it was very thin ( $\sim 50 \text{ nm}$ ). The principal diffraction lines were (112), (204)/(220), and (116)/(312) from the  $\text{CuInSe}_2$  chalcopyrite phase. The preferred orientation for sample 1 that was estimated from the intensity ratio of the  $\text{In}_{112}/\text{In}_{204,220}$  reflections was  $\sim 3.1$ , which indicated that the grains were primarily oriented along the  $\langle 112 \rangle$  direction. Reflections near angles  $2\theta \sim 41^\circ$  and  $2\theta \sim 74^\circ$  were due to reflection from the Mo film on the glass substrate.

Optical characteristics of standard CIGS films on glass were determined from measurements of the transmittance ( $T$ ) and reflection coefficient ( $R$ ). The transmission spectra (Fig. 4a) showed that sample 2 had a relatively high transmittance ( $\sim 70\%$ ) in the near-IR region and a clearly defined interference structure that was characteristic of high-quality CIGS films. The relatively sharp fundamental absorption edge of CIGS film was clearly visible in the square of the absorption coefficient as a function of the photon-energy spectrum (Fig. 4b). These experimental results confirmed that CIGS films grown on glass had a relatively high quality. The reflection coefficient of polycrystalline CIGS films measured in the spectral range  $\sim 0.8$ – $1.4 \text{ eV}$  was  $\sim 0.18$  for sample 2. The film absorption coefficient was calculated using the following expression [11]:

$$\alpha = \frac{1}{d} \ln \frac{\sqrt{(1-R)^4 + 4T^2R^2} + (1-R)^2}{2T}, \quad (1)$$

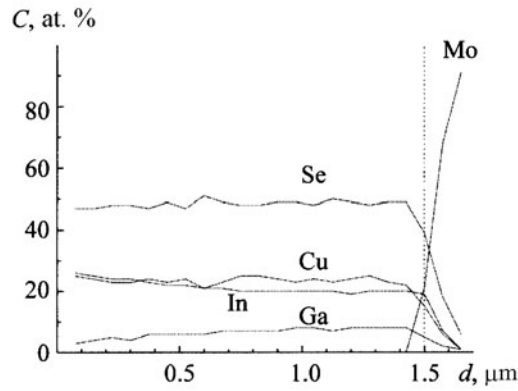


Fig. 1. Element distribution profiles with CIGS film depth for sample 1.

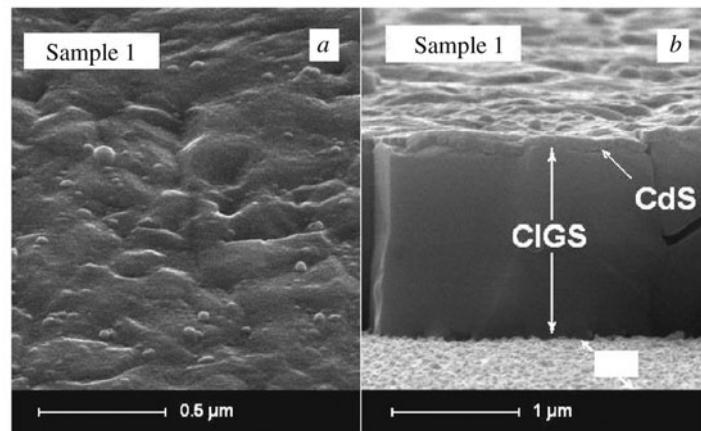


Fig. 2. Surface morphology (a) and a portion of chip cross-section (b) for CdS/CIGS/Mo/glass heterostructure.

where  $d$  is the film thickness. The absorption coefficient for resolved direct transitions as a function of the spectrum was determined from the equation [12]:

$$\alpha(h\nu) = A(h\nu - E_g)^{1/2}, \quad (2)$$

where  $A$  is a constant;  $E_g$ , the band-gap width. The band-gap width for CIGS films was determined by extrapolating the linear part of the curve  $\alpha^2 = f(h\nu)$  to the photon-energy axis at 300 and 4.2 K and gave  $E_g = 1.22$  and 1.28 eV (Fig. 4b). These  $E_g$  values agreed satisfactorily with experimental results from other research groups for CIGS films with a similar chemical composition [13, 14]. Because the Mo contact layer was opaque so that the transmittance of the CdS/CIGS/Mo/glass structures could not be measured, the band-gap width  $E_g$  was determined by measuring photoluminescence excitation (PLE) spectra. Figure 5a shows photoluminescence (PL) and PLE spectra measured at 4.2 K for CdS/CIGS/Mo/glass heterostructures (sample 1) before irradiation (spectrum 1) and after irradiation with electrons at a dose of  $5 \cdot 10^{17} \text{ cm}^{-2}$  (spectra 2–4). Similar spectra were recorded for sample 2, which was formed directly on the glass substrate. The position of maxima in the PLE spectra corresponded to energies  $\sim 1.26$ – $1.30$  eV, which is close to the  $E_g$  value found from absorption data for sample 2 with practically the same chemical composition as sample 1 (Table 1). We note that PLE spectra were recorded with detection near the maxima of the three principal luminescence bands ( $E_{\text{rec}}$ ): a band due to donor–acceptor-type (D–A) optical transitions at  $\sim 1.052$  eV and bands  $P_1$ ,  $\sim 0.91$  eV, and  $P_2$ ,  $\sim 0.77$  eV, due to recombination of non-equilibrium charge carriers through deep energy levels of radiation defects. Figures 5 and 6 show that PL spectra of unirradiated CIGS films at 4.2 K contained a single band at 1.052 eV

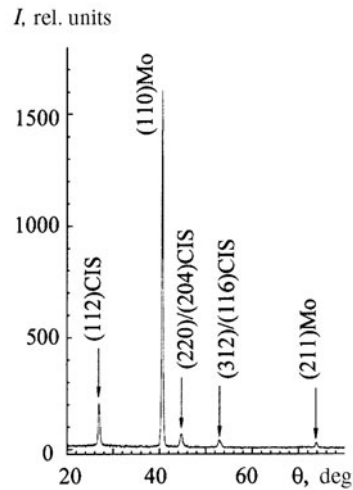


Fig. 3. X-ray diffraction pattern of CdS/CIGS/Mo/glass heterostructure.

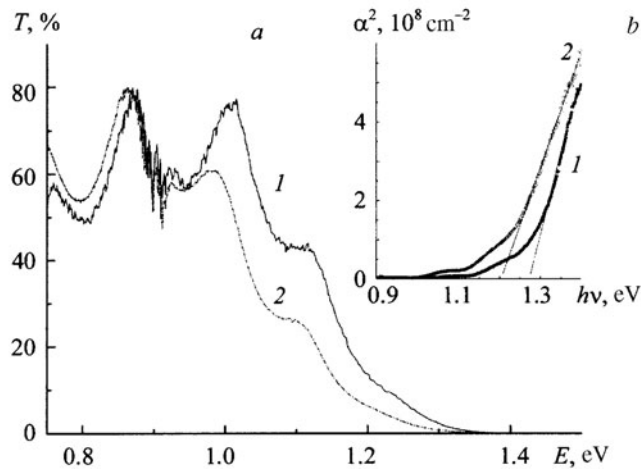


Fig. 4. Transmission (a) and absorption (b) spectra of sample 2 at 4.2 (1) and 300 K (2).

with half-width  $\sim 55$  meV. This band shifted to higher energies by 12 meV and the intensity changed by an order of magnitude ( $j$ -shift) as the excitation level increased from 0.006 to 2 W/cm<sup>2</sup>. The spectral shape of the D–A band practically did not change during this (Fig. 6). The relatively large spectral shift of the band at 1.052 eV from the band-gap width  $E_g \sim 1.28$  eV, a total of  $\sim 0.23$  eV, and the high-energy shift of this band as a function of the excitation level were consistent with D–A recombination with a strong influence of potential fluctuations [15]. Practically symmetric D–A bands of analogous spectral shape near 1.00 and 1.04 eV with half-width  $\sim 76$  and 85 meV, respectively, were observed at 2 K in PL spectra of CIGS films with a Ga/(Ga+In) concentration ratio  $\sim 0.25$  [16]. Symmetric D–A bands, the maxima of which were located at 1.03–1.05 eV and the half-width of which changed in the range 50–80 meV with electron-beam surface scanning of separate crystallites, were observed at 15 K in cathodoluminescence spectra of polycrystalline CIGS films [17]. It is important to note that the spectral shape of broad D–A bands was practically constant at relatively low excitation levels changing over two orders of magnitude. Almost symmetric D–A bands were observed in other work also [18, 19]. In our opinion, the D–A bands in PL spectra of CIGS films were not asymmetric because the probability of interaction of electrons with  $LO$ -phonons ( $\sim 28$  meV) during D–A optical transitions was significantly reduced owing to the presence of significant potential fluctuations in the crystal matrix.

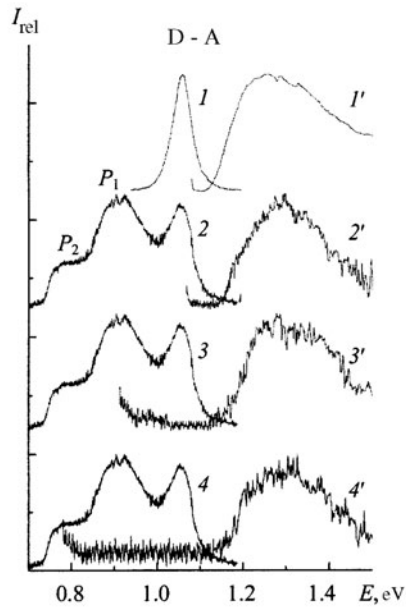


Fig. 5. Photoluminescence (1-4) and photoluminescence excitation (1'-4') spectra at 4.2 K of CdS/CIGS/Mo/glass structures before (1) and after (2-4) irradiation;  $E_{rec} \sim 1.06$  (1', 2'), 0.91 (3'), and 0.78 eV (4').

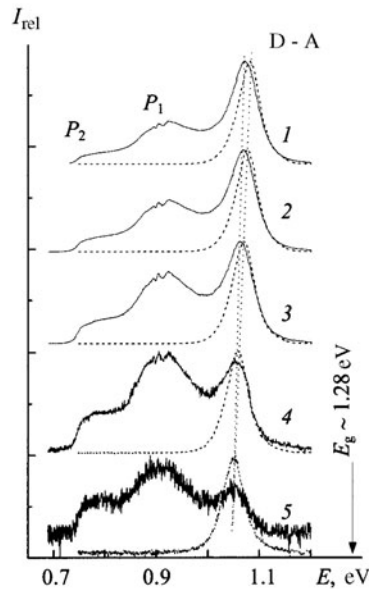


Fig. 6. Photoluminescence spectra of CdS/CIGS/Mo/glass structures at 4.2 K as a function of excitation level ( $W/cm^2$ ): 0.006 (1), 0.028 (2), 0.26 (3), 0.78 (4), 2.0 (5); solid lines, after irradiation; dashed lines, before irradiation.

Thus, the probability of phonon-less transitions did not change. The D-A recombination band was assumed to be related to recombination at Cu vacancies ( $V_{Cu}$ ) as acceptors and Se vacancies ( $V_{Se}$ ) or In atoms replacing Cu ( $In_{Cu}$ ) as deep donors according to a theoretical calculation of the position of the energy levels of these defects in the band gap and experimental results obtained from  $CuInSe_2$  using various physical methods [20, 21]. A D-A band with a maxi-

mum at  $\sim 1.05$  eV was also assigned to these types of growth point defects (donors and acceptors) in previous studies [16, 17].

Experiments on irradiation of CIGS films with high-energy electrons ( $\sim 5$  MeV) showed that the short-wavelength shift of the 1.052-eV band as a function of excitation level decreased up to 8 meV for an order of magnitude change of the excitation intensity at an irradiation dose of  $\sim 5 \cdot 10^{17}$  cm $^{-2}$  (Fig. 6). In our opinion, the decrease in the shift from 12 to 8 meV was due to a reduction in the amplitude of potential fluctuations in the crystal lattice of irradiated chalcopyrite CIGS films [15]. This reduction may have been related to effective interaction of radiation-induced defects with growth defects. As a result, certain growth defects were apparently "cured" by point defects formed during electron irradiation, i.e., the total concentration of defects and the compensation level of donors and acceptors both in separate grains and at interfaces between them in the polycrystalline CIGS layer were reduced [15]. It is important to note that the parameters of solar elements based on CIGS films were found to improve after irradiation with 1-MeV electrons at doses  $\geq 10^{16}$  cm $^{-2}$  [22]. Our results also demonstrated a positive effect of electron irradiation at doses  $< 5 \cdot 10^{17}$  cm $^{-2}$  that was evident in an ordering of the crystal structure of CIGS films owing to curing of growth defects. Furthermore, the integrated intensity of the D–A band at  $\sim 1.052$  eV increased by 2–4 times upon increasing the electron-irradiation dose from  $10^{16}$  to  $10^{17}$  cm $^{-2}$ . This was due to an increase in the lifetime of non-equilibrium charge carriers due to curing by radiation defects of radiationless recombination channels, i.e., growth defects. It is important to note that similar effects in optical luminescence spectra were observed upon irradiation of CIGS films by deuterons and protons [15, 23, 24].

In addition to this, irradiation of CIGS films produced two additional deep bands  $P_1$  at  $\sim 0.91$  eV and  $P_2$  at  $\sim 0.77$  eV in the PL spectra (Figs. 5 and 6). High irradiation doses ( $\geq 5 \cdot 10^{17}$  cm $^{-2}$ ) decreased the intensity of the principal D–A band whereas those of the  $P_1$  and  $P_2$  bands, which were due to radiation-induced defects, continued to increase. These bands did not shift as a function of excitation level and corresponded to optical transitions into energy levels of deep defects at  $\sim 0.37$  and 0.51 eV in the CIGS band gap. In our opinion, defects induced by electron irradiation are the simplest point defects, Cu atoms replacing In  $\text{Cu}_{\text{In}}$  ( $P_1$  band) and In vacancies  $\text{V}_{\text{In}}$  ( $P_2$  band) [20].

**Conclusion.** The band-gap energy of thin films of semiconducting CIGS compounds with a Ga/(Ga + In) ratio  $\sim 0.27$  was determined as  $E_g \sim 1.28$  eV at 4.2 K based on optical properties (transmission, reflectance, PL, and PLE spectra). It was found that irradiation of CIGS thin films by high-energy ( $\sim 5$  MeV) electrons at doses  $10^{16}$ – $2 \cdot 10^{18}$  cm $^{-2}$  produced radiation defects that were effective channels for radiationless recombination with deep energy levels  $\sim 0.37$  and 0.51 eV in the band gap of the material. It was hypothesized that Cu atoms replacing In  $\text{Cu}_{\text{In}}$  and In vacancies  $\text{V}_{\text{In}}$  were responsible for the appearance of the levels at 0.37 and 0.51 eV. A curing of growth defects by radiation-induced defects that led to decreased potential fluctuations in CIGS films was observed. This was evident in a decreased shift of the D–A recombination band at  $\sim 1.052$  eV by 1.5 times (from 12 to 8 meV) as the excitation level changed by an order of magnitude. Also, the integrated intensity of this band increased at irradiation doses  $\leq 10^{17}$  cm $^{-2}$ . The observed effects improved the structure and quality of the CIGS films. This suggests that electron irradiation at low doses ( $5 \cdot 10^{17}$  cm $^{-2}$ ) will also improve the parameters of solar cells formed from CIGS compounds with the chalcopyrite structure.

**Acknowledgments.** The work was supported by the State Complex Research Program Nanomaterials and Nanotechnology, task 6.17, Royal Society of Great Britain (Project IJP 2008/R1) and EPSRC (Project EP/E026451/1).

## REFERENCES

1. I. Repins, M. A. Contreras, B. Egaas, C. DeHart, J. Scharf, and C. L. Perkins, *Prog. Photovolt. Res. Appl.*, **16**, 235–239 (2008).
2. P. Jackson, R. Wurz, U. Rau, J. Mattheis, M. Kurth, T. Schlotzer, G. Bilger, and J. H. Werner, *Prog. Photovolt. Res. Appl.*, **15**, 507–519 (2007).
3. S. Messenger, R. Walters, G. Summers, T. Morton, G. La Roche, C. Signorini, O. Anzawa, and S. Matsuda, *Proc. 16th Eur. PV Solar Energy Conference*, Glasgow, UK (2000), 974–977.
4. A. Jasenek and U. Rau, *J. Appl. Phys.*, **90**, 650–658 (2001).
5. H. S. Lee, H. Okada, A. Wakahara, and A. Yoshida, *J. Appl. Phys.*, **94**, 276–278 (2003).
6. A. V. Mudryi, A. V. Ivanyukovich, M. V. Yakushev, Ya. V. Feofanov, V. S. Kulikauskas, and V. S. Chernysh, *Poverkhnost*, **4**, 51–54 (2006).

7. T. Schlenker, V. Laptev, H. W. Schock, and J. H. Werner, *Thin Solid Films*, **480–481**, 29–32 (2005).
8. G. Hanna, J. Mattheis, V. Laptev, Y. Yamamoto, U. Rau, and H. W. Schock, *Thin Solid Films*, **431–432**, 31–36 (2003).
9. G. Hanna, A. Jasenek, U. Rau, and H. W. Schock, *Phys. Status Solidi A*, **179**, R7–R8 (2000).
10. A. V. Mudryi, A. V. Ivanyukovich, M. V. Yakushev, R. Martin, and A. Saad, *Zh. Prikl. Spektrosk.*, **74**, No. 3, 373–377 (2007).
11. H. Neumann, W. Horig, P. A. Jones, G. Lippold, H. Sobotta, R. D. Tomlinson, and M. V. Yakushev, *Cryst. Res. Technol.*, **29**, 719–726 (1994).
12. J. I. Pankove, *Optical Processes in Semiconductors*, Prentice-Hall, Englewood Cliffs, New Jersey (1971).
13. G. W. el Haj Moussa, M. Ajaka, M. El Tahchi, E. Eid, and C. Llinares, *Phys. Status Solidi A*, **202**, 469–475 (2005).
14. S. Theodoropoulou, D. Papadimitriou, N. Rega, S. Siebentritt, and M. C. Lux-Steiner, *Thin Solid Films*, **511–512**, 690–694 (2006).
15. M. V. Yakushev, R. W. Martin, J. Krustok, A. V. Mudryi, D. Holman, H. W. Shock, R. D. Pilkington, A. E. Hill, and R. D. Tomlinson, *Thin Solid Films*, **378**, 201–204 (2001).
16. V. Alberts, J. H. Schon, M. J. Witcomb, E. Bucher, U. Ruhle, and H. W. Shock, *J. Phys. D: Appl. Phys.*, **31**, 2869–2876 (1998).
17. M. J. Romero, K. Ramanathan, M. A. Contreras, M. M. Al-Jassim, R. Noufi, and P. Sheldon, *Appl. Phys. Lett.*, **83**, 4770–4772 (2003).
18. T. Enzenhofer, T. Unold, and H. W. Shock, *Phys. Status Solidi A*, **203**, 2624–2629 (2006).
19. K. Yoshino, M. Iwamoto, H. Yokoyama, A. Fukuyama, K. Maeda, S. Niki, and T. Ikari, *Jpn. J. Appl. Phys.*, **38**, 3171–3714 (1999).
20. S. B. Zhang, S. H. Wei, A. Zunger, and H. Hatayama-Yoshida, *Phys. Rev. B: Condens. Matter Mater. Phys.*, **57**, 9642–9656 (1998).
21. C. Rincon and R. Marquez, *J. Phys. Chem. Solids*, **60**, 1865–1873 (1999).
22. A. Jasenik, T. Hahn, M. Schmidt, K. Weinert, M. Wimbor, G. Hanna, K. Orgassa, M. Hartmann, H. W. Schock, U. Rau, J. H. Werner, B. Schattat, S. Kraft, K. H. Schmid, W. Bolse, G. Laroche, A. Robben, and K. Bogus, in: *Proc. 16th Eur. PV Solar Energy Conference*, Glasgow, UK (2000), 982–986.
23. A. V. Mudryi, A. V. Ivanyukovich, M. V. Yakushev, V. S. Kulikauskas, and V. S. Chernysh, *Zh. Prikl. Spektrosk.*, **73**, No. 6, 828–830 (2006).
24. M. V. Yakushev, R. W. Martin, F. Urquhart, A. V. Mudryi, H. W. Shock, J. Krustok, R. D. Pilkington, A. E. Hill, and R. D. Tomlinson, *Jpn. J. Appl. Phys.*, **39**, Suppl. 39-1, 320–321 (2000).